



Sorption of phenol from synthetic aqueous solution by activated saw dust: Optimizing parameters with response surface methodology



Omprakash Sahu^{a,*}, Dubasi Govardhana Rao^a, Nigus Gabbiye^a, Addis Engidayehu^a,
Firomsa Teshale^b

^a School of Chemical and Food Technology, Bahir Dar Institute of Technology, BDU, Ethiopia

^b School of Chemical and Bio-Engineering, Addis Ababa Institute of Technology, Addis Ababa, Ethiopia

ARTICLE INFO

Keywords:

Adsorption
Bio-waste material
Phenol
Saw dust
Wastewater treatment

ABSTRACT

Organic pollutants have an adverse effect on the neighboring environment. Industrial activities are the major sources of different organic pollutants. These primary pollutants react with surrounding and forms secondary pollutant, which persists for a long time. The present investigation has been carried out on the surface of activated sawdust for phenol eliminations. The process parameters initial concentration, contact time, adsorbent dose and pH were optimized by the response surface methodology (RSM). The numerical optimization of sawdust (SD), initial concentration 10 mg/l, contact time 1.5 h, adsorbent dose 4 g and pH 2, the optimum response result was 78.3% adsorption. Analysis of variance (ANOVA) was used to judge the adequacy of the central composite design and quadratic model found to be suitable. The coefficient of determination values was found to be maximum Adj R² 0.7223, and Pre R² 0.5739 and significant regression at 95% confidence level values.

1. Introduction

Phenol is an essential industrial solvent for different production concern. In cooperation with its position under 595 hazardous wastes among 1678 listed on Environmental Protection Agency National Priorities List [1]. Phenol is available in air, water, and soil by industrial activities and natural deterioration of organic wastes. Phenol degraded rapidly in air and soil by hydroxyl radical reaction (estimated half-life 14.6 h), and persist in water for a somewhat longer period [2]. If degradation is sufficiently slow, phenol in sunlight water will undergo photooxidation with photochemically produced peroxy radicals, and leach to groundwater [3]. The most common anthropogenic sources of phenol in water include coal tar [4], waste water from processing industries such as resins [5], plastics [6], fibers [7], adhesives [8], iron and steel [9], leather [10], paper pulp mills [11] and wood treatment facilities [12]. The addition of this there is two natural sources of phenol in aquatic media are animal wastes and decomposition of organic wastes [13].

In literature, aqueous phenolic wastes have been treated for many years by different methods including chemical oxidation [14], chemical coagulation [15], extraction with solvents [16,17], membrane technology [18], ion exchange [19] and adsorption [20,21]. Among them, physical adsorption method is generally considered to be the best,

effective, economical and most frequently used method for the removal of phenolic pollutions [22]. Different types of synthetic and natural adsorbents have been used to treat the phenolic wastewater by researchers [23]. Attention has been focused on natural adsorbents (bacteria, fungi, yeast, algae, agricultural by-products, and wood by-products), which have good absorption capacities due to large surface area, homogeneous pore size, well defined structural properties, selective adsorption ability, easy regeneration, and multiple uses [24]. Adsorbent methods has been also applied for removal of DDT [25], cyanide [26], copper [27], mercury [28], color dye [29] etc. Among them waste biomass consider to be easily available in almost all region with reasonable price. The major component of biomass like lignin, cellulose and hemicellulose provides large surface area and better attachment with aromatic organic compound [26,29].

The main aim of this research work is to subtract the phenol from synthesized wastewater by adsorbent technique. The experiment was performed in the batch reactor. The effect of different experimental parameters such as the solution pH, temperature, sorbate concentration on the adsorption has been optimized by using response surface methodology. The interaction between phenol molecules and activated surface has been studied with Langmuir isotherm. The characterisations of adsorbent and adsorbed were also studied with Fourier transfer infrared (FTIR), energy diffractive x-ray (EDX-ray) and scanning electron

* Corresponding author.

E-mail address: ops0121@gmail.com (O. Sahu).

<http://dx.doi.org/10.1016/j.bbrep.2017.08.007>

Received 19 December 2016; Received in revised form 11 July 2017; Accepted 16 August 2017

Available online 24 August 2017

2405-5808/ © 2017 The Authors. Published by Elsevier B.V. This is an open access article under the CC BY-NC-ND license (<http://creativecommons.org/licenses/by-nc-nd/4.0/>).

micrographic (SEM).

2. Material and methods

2.1. Materials

2.1.1. Chemical and water sample

All the analytical grade chemicals were used in this experiment supplied by Himedia Laboratories Pvt. Ltd. Mumbai India. A stock solution containing 1000 mg/L of phenol was prepared by dissolving 1 g of pure phenol crystal in 1 L of Millipore water (Q-H₂O, Millipore Corp. with a resistivity of 18.2 MX-cm).

2.1.2. Adsorbent

The sawdust was arranged from the local timber industry and washed with distilled water to remove the dust particles. To prevent the color leaching and other impurities sawdust were washed until clear solution obtained. Finally, washed biosorbent was dried at 75 °C in the oven for 8 h. To prepared activated carbon, dried sawdust mixed with 2 N H₂SO₄ in 1:3 solid to liquid ratio and kept in a muffle furnace at temperature 200 °C for 14 h. The sawdust activated carbon was washed with millipore water to eliminate residual chemicals and dried at 60 °C temperature for 24 h. Additional soaking has been done with 1% NaHCO₃ solution and kept overnight for the complete elimination of acid. The product was washed with double distilled deionized water until superficial liquid were acquired and dried at 60 °C for 12 h. Finally, the adsorbent was stored in an airtight poly bag for the experiment. The physicochemical characteristics of activated sawdust are mention in Table 1.

2.2. Methods

2.2.1. Experimental design

The parameters initial concentration (IC), contact time (CT), adsorbent dosage (AD) and pH on adsorption efficiency with sawdust was studied with a standard response surface methodology (RSM) design called central composite design (CCD). This method helps to optimize the effective parameters with a minimum number of experiments, and also to analyze the interaction between the parameters [30]. In this study percentage adsorption has been taken as a response (Y) of the system, while process parameters, initial concentration 5–40 mg mL⁻¹; pH: 2–10; Contact time 1–3 h and adsorbent dose 0.5–5 g has been taken as input parameters. For statistical calculations, the levels for the four main variables X₁(IC), X₂(t), X₃(g) X₄(pH) were coded as according to the following relationship.

$$x_i = \frac{(X_i - X_0)}{\delta X} \quad (1)$$

where X₀ is the value of X_i at the center point and δX presents the step change. The variables and levels of the design model are given in Table 2. The results of the Y (response) of adsorption were measured according to design matrix listed in Table 3. From experimental observations, it was assumed that the higher order interactions were small

Table 1
Characteristics of activated sawdust.

S.No	Characteristics	Values
1	Specific gravity	0.61
2	Bulk density (Kg/m ³)	415
3	Porosity (%)	72
4	Mean pore radius (Å)	4.5
5	Surface area (m ² /g)	19
6	Moisture content (%)	50.1
7	Loss on ignition (w/w %)	96.12
8	BET surface area (m ² /g)	910

Table 2
Factors and levels of the experimental design for adsorption.

Factors	Level 1 (-α)	Level 2 (-1)	Level 3 (0)	Level 4 (+1)	Level 5 (+α)
Inlet concentration (mg/l)	5	10	20	30	40
pH	2	4	7	8	10
Contact Time (h)	1	1.5	2	2.5	3
Adsorbent Dose (g)	0.5	1	3	4	5

Table 3
The different combination of the factors for the experimental design.

Runs	X ₁ (Initial Concentration)	X ₂ (Contact Time)	X ₃ (adsorbent dose)	X ₄ pH	Y (% adsorption)
1	0	0	0	0	73
2	0	0	0	-2	82
3	1	-1	1	1	91
4	-1	-1	1	-1	96
5	0	0	0	0	67
6	-1	1	-1	-1	74
7	-1	1	1	1	97
8	0	0	0	0	67
9	-2	0	0	0	81
10	0	0	0	0	67
11	0	0	0	0	67
12	1	1	1	-1	85
13	-1	-1	1	1	51
14	2	0	0	0	55
15	0	0	0	2	9
16	-1	-1	-1	1	92
17	1	1	-1	1	47
18	0	0	0	0	67
19	1	-1	-1	1	71
20	1	-1	1	-1	53
21	0	0	-2	0	30
22	-1	1	-1	1	92
23	1	1	-1	-1	75
24	-1	-1	-1	-1	93
25	0	-2	0	0	30
26	1	1	1	1	32
27	-1	1	1	-1	92
28	1	-1	-1	-1	55
29	0	2	0	0	67
30	0	0	2	0	91

relative to the low order.

2.2.2. Experiment

The sorption of phenol on sawdust was studied in a batch mode at room temperature. The kinetic adsorption experiments were carried out in 100 mL flasks sealed with Parafilm, to prevent the loss of phenol by volatilization. The general method has been used for this study. A known weight of sawdust was equilibrated with 60 mL of the phenol solution (known concentration) at room temperature of 21 °C for a known period of time (Table 3). All adsorption studies were conducted in a rotary incubator shaker at agitation speed (Sa) of 150 rpm. The flasks were then removed from the shaker and the final concentration of phenol in the solution was analyzed using a spectrophotometer UV. The pH of the suspension in the experiments was adjusted with NaOH 0.1 M (1 M) and H₂SO₄ 0.1 M (1 M). In addition, for the reliability of adsorption data, blank tests were also carried out in the same way.

The adsorption efficiency of phenol in solution was calculated by equation:

$$\text{Removal}(\%) = \frac{(C_0 - C_e) \times 100}{C_0} \quad (2)$$

The phenol concentration retained on the adsorbent phase (q mg mg⁻¹) was calculated by equation:

$$q = \frac{V(C_0 - C)}{W} \tag{3}$$

where C_0 (mg mL^{-1}) and C (mg mL^{-1}) are the concentrations of phenol before and after adsorption reaction, respectively, V (mL) is the volume of the reaction solution, and W (g) is the adsorbent mass.

2.2.3. Analysis of sample

Fourier transform infrared (FTIR) spectroscopic analysis was performed (FTIR-2000, Perkin Elmer). The spectra were measured from 4000 to 0 cm^{-1} . The surface area, total pore volume, and average pore diameter of the samples were determined from the adsorption isotherms of nitrogen at 77 K using Autosorb I, supplied by Quanta chrome Corporation, USA. The surface morphology of the sample was examined using scanning electron microscope (Model VPFESEM Supra 35VP). Proximate analysis was carried out using thermogravimetric analyzer (TGA) (Model Perkin Elmer TGA7, USA).

3. Result and discussion

3.1. Model fitting and statistical analysis

The percentages of adsorption (Y) affecting parameters were optimized by central composite design and response surface method. In order to describe the nature of the response surface in the optimum region, a central composite design with five coded levels ($-\alpha, -1, 0, +1, +\alpha$) was performed and four factors (IC, CT, AD and pH) were selected using design expert 6.0.8 software and processed. The results of the Y (response) of adsorption were measured according to design matrix and the measured responses are listed in Table 3. Linear, interactive, quadratic and cubic models were fitted to the experimental data to obtain the regression equations. Two different tests namely the sequential model sum of squares and model summary statistics were employed to decide about the adequacy of various models to represent adsorption with sawdust. Results of these tests are given in Tables 4 and 5, for percentage adsorption removal respectively. The cubic model was found to be aliased. For quadratic and linear models, the p -value was lower than 0.02, and both of these could be used for further study as per sequential model sum of squares test. As per model summary statistics, the quadratic model was found to have maximum Adj R^2 0.7223, and Pre R^2 0.5739 values excluding cubic model which was aliased. Therefore, a quadratic model was chosen for further analysis. To determine whether or not the quadratic model is significant, it is crucial to perform analysis of variance (ANOVA) mention in Table 6. The probability (P -values) values are used as a device to check the significance of each coefficient, which also shows the interaction strength of each parameter (smaller the P -values bigger significance of the corresponding coefficient). In addition to analyzing the independent variables' effects, this experimental methodology also generates a mathematical model. The graphical viewpoint of the mathematical model has led to the term RSM. The relationship between the responses and the

Table 4
S0065quential model sum of squares.

Source	Sum of Squares	Df	Mean Square	F Value	p-value Prob > F	Remark
Mean vs Total	139946.7	1	139946.7			Suggested
Linear vs Mean	4586.333	4	1146.583	2.814678	0.0468	Suggested
2FI vs Linear	819.75	6	136.625	0.277212	0.9407	
Quadratic vs 2FI	661.05	4	165.2625	0.284832	0.8832	
Cubic vs Quadratic	6342.167	8	792.7708	2.350443	0.1385	Aliased
Residual	2361	7	337.2857			
Total	154717	30	5157.233			

*Sequential Model Sum of Squares Selects the highest order polynomial where the additional terms are significant and the model is not aliased.

inputs is given in equation

$$Y = f(X_1, X_2, X_3, X_4, \dots, X_n) \pm \epsilon \tag{4}$$

where:

- Y is the response;
- f is the unknown function of response,
- $X_1, X_2, X_3, \dots, X_n$ are the input variables, which can affect the response,
- n is the number of the independent variables, and
- ϵ is the statistical error that represents other sources of variability not accounted for by f .

After selection of the design, the model equation is defined and coefficients of the model equation are predicted. A manual regression method was used to fit the second order polynomial given by Eq. (5), respectively to the experimental data and to identify the relevant model terms. The final equation obtained in terms of coded factors is given below:

$$\begin{aligned} \% \text{Adsorption}(Y) = & 68.3 - 9.5833 \times X_1 + 2.75 \times X_2 + 5 \times X_3 \\ & - 8.1667 \times X_4 \end{aligned} \tag{5}$$

The statistical significance of the ratio of mean square variation due to regression and mean square residual error was tested using ANOVA [31]. The ANOVA for the second-order equation fitted for percentage adsorption efficiency. The Model F-value of 2.81 implies the model is significant. There is only a 4.68% chance that a "Model F-Value" could occur due to noise. Values of "Prob > F" less than 0.0500 indicate model terms are significant. In this case, X_1 and X_3 are significant model terms. Values greater than 0.1000 indicate the model terms are not significant which are contact time and pH.

3.1.1. Significance of experimental parameters

The effect of contact time on the percentage adsorption of phenol at optimum conditions is the presented in Fig. 1. It was observed that the equilibrium time is dependent on the adsorbate concentration. As the time period for which the adsorbent was kept in contact with phenol solution was increased, the percentage adsorption increasing and reached equilibrium at 1.5 h for 5 mg/l and 10 mg/l, 2 h for 20 mg/l and 30 mg/l, 2.5 h for 40 mg/l respectively. This might be due to the active binding sites of adsorbent fully bind the ions up to 1.5 to 2 h and after this time there was no change in percentage adsorption. Since the adsorption process is a transfer of the pollutant from the liquid phase to the solid one, the contacting time between the two phases has an effect on the mass transfer rate. So the above mentioned times are the best time for adsorption. The experimental result of sorption of phenol on sawdust at various concentrations is shown in Fig. 2. Studied showed that the percentage adsorption decreased with increase in the initial concentration of the pollutant. The extent of adsorption increased from 46% to 86% when the concentration of the adsorbate decreased from 40 mg/l to 5 mg/l. The increase in uptake may be due to the availability of more number of phenol ions in solution for sorption. Moreover, higher initial adsorbate concentration provided higher driving force to overcome all mass transfer resistances of the ions from the aqueous to the solid phase resulting in higher probability of collision between ions and the active sites [32].

The effect of pH value on the percentage removal of phenol at optimum values of the others factor is shown Fig. 3. It can be seen that the percentage adsorption is higher at lower pH. As the pH increased, there was little increase in the percentage of adsorption and it was maximum at pH 4. This may be due to the molecular form of phenol persists in the medium and surface protonation is minimum, leading to the enhancement of phenol adsorption. When the pH was further increased, a sharp decrease in the percentage of adsorption was observed. It attributes to the weakening of electrostatic force of attraction between the

Table 5
Model summary statistics.

Source	Std.	Adjusted		Predicted		Remark
	Dev.	R-Squared	R-Squared	R-Squared	PRESS	
Linear	0.004591	0.76614	0.7222912	0.5738805	0.000614	Suggested
2FI	0.004937	0.7803154	0.6789225	-0.3737402	0.001981	
Quadratic	0.005352	0.8013884	0.622638	-0.7369903	0.002505	Aliased
Cubic	0.002031	0.9828329	0.9456376	-2.7842138	0.005457	

Table 6
Analysis of variance.

Source	Sum of Squares	Df	Mean Square	F Value	p-value Prob > F	Remark
Model	4586.333	4	1146.583	2.814678	0.0468	significant
X ₁	2204.167	1	2204.167	5.410875	0.0284	
X ₂	181.5	1	181.5	0.445553	0.5106	
X ₃	600	1	600	1.472903	0.02362	
X ₄	1600.667	1	1600.667	3.929379	0.0585	
Residual	10183.97	25	407.3587			
Lack of Fit	10153.97	20	507.6983	84.61639		
Pure Error	30	5	6			
Cor Total	14770.3	29				

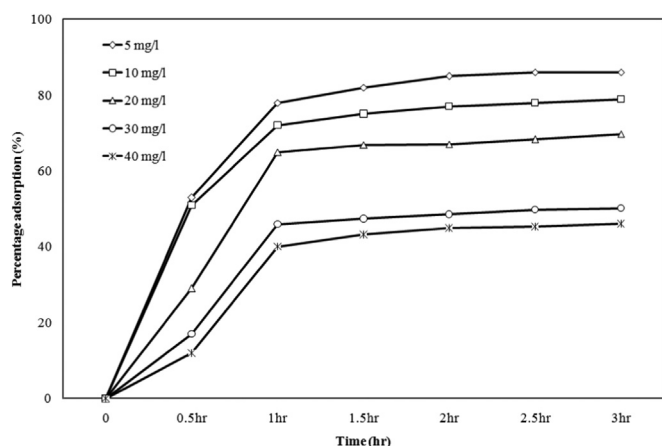


Fig. 1. Effect of initial concentration of phenol on contact time.

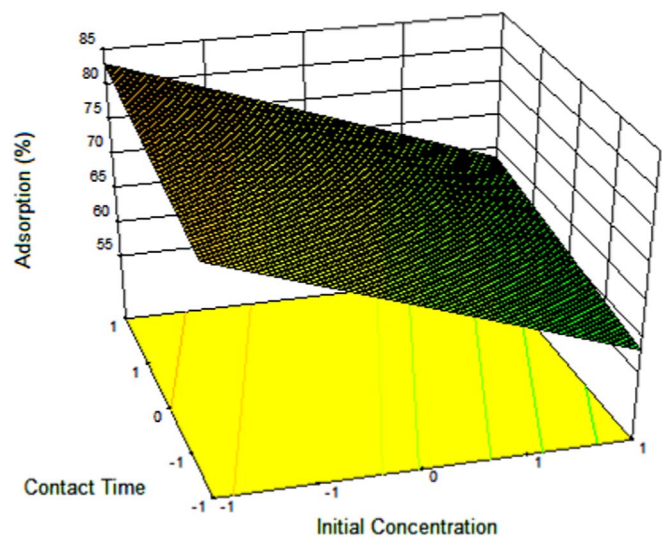


Fig. 2. Effect of initial concentration of phenol on contact time.

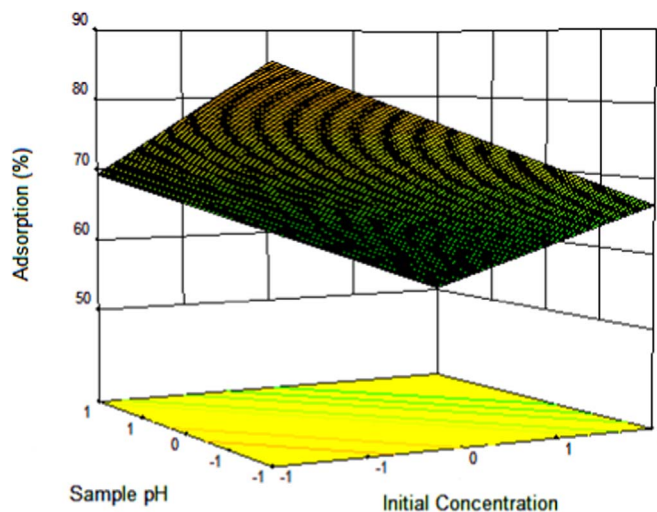


Fig. 3. Effect of initial concentration of phenol on pH.

oppositely charged adsorbate and adsorbent and ultimately led to the reduction in sorption capacity [33]. When the pH was increased beyond 7.0, a gradual decrease in the percentage adsorption was observed. This might be due to the in high pH range, phenol forms salts which are readily ionized leaving the negative charge on the phenolic group. At the same time, the presence OH⁻ ions on the adsorbent prevents the uptake of phenolate ions. In acidic medium, the H⁺ ions on the surface are also exchanged with the positively charged sorbet species with subsequent coordination of phenol ion. The decrease in the removal of ions at higher pH (≤ 4) is apparently due to the higher concentration of H⁺ ions present in the reaction mixture, which compete with the ions for the adsorption sites of sawdust and formation of soluble hydroxyl complexes. Similar behavior has been reported during the adsorption using rice husk [34], agriculture waste [35] and activated carbon [36].

The percentage adsorption increased with increase in adsorbent dose. This shows in Fig. 4 where the percentage adsorption was plotted against adsorbent dose. The percentage adsorption increased from 45% (minimum) at a lower adsorbent dose to 86% (maximum) at a higher adsorbent dose. This can be attributed to increased adsorbent surface area and availability of more adsorption sites resulting from the increasing adsorbent dosage. Further increase in adsorbent dose decreases the adsorption. The decrease in phenol ion uptake at higher adsorbent dose may be due to the competition of the ions for the sites available [37].

For numerical optimization of sawdust (SD), the optimum response result was 78.3%, percentage adsorption. The optimum processing conditions using numerical optimization were the coded levels (-1, -1, 1, -1) or initial concentration (10 mg/l), contact time (1.5 h), adsorbent dose (4 g) and pH (2) and is shown in Fig. 5(a). The Response prediction desirability is found to be very good 0.942, shown in Fig. 5(b).

3.1.2. Adsorption equilibrium

Langmuir isotherm model is probably the most widely applied

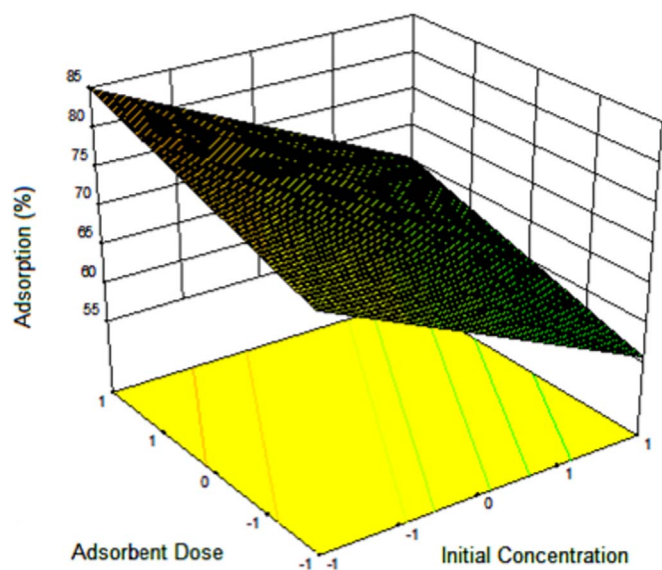


Fig. 4. Effect of initial concentration of phenol on adsorbent dose.

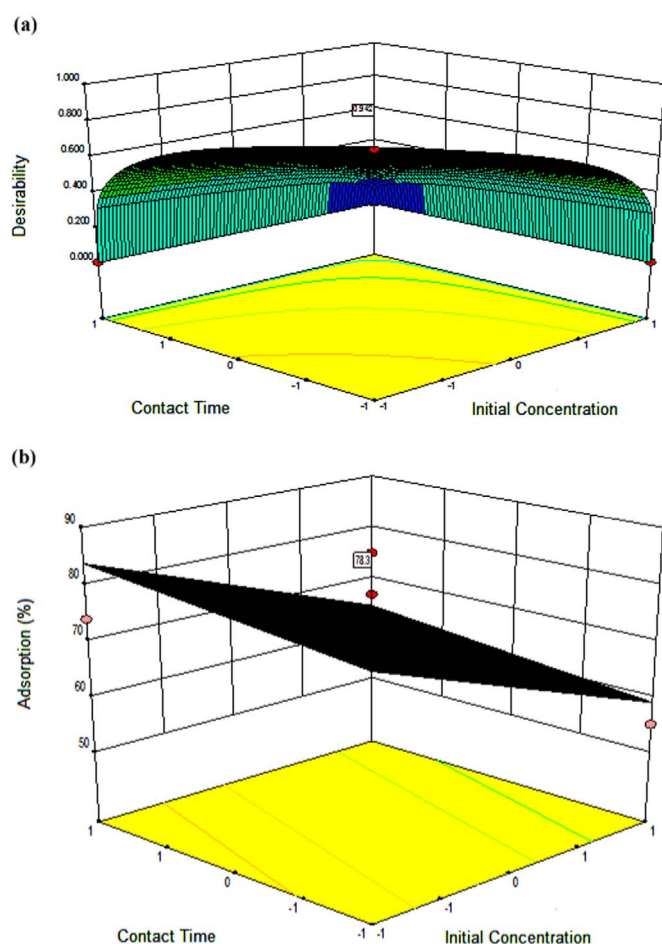


Fig. 5. Graphic representation of the (a) desirability 3D plot (b) optimized percentage adsorption for sawdust.

model for isotherm adsorption. It considers the adsorption energy of each molecule is the same, independent of the surface of material, the adsorption takes place only on some sites and there are no interactions between the molecules. The Langmuir equation was used to study the adsorption isotherms of phenol. The linear form of the Langmuir equation [38] is as follows:

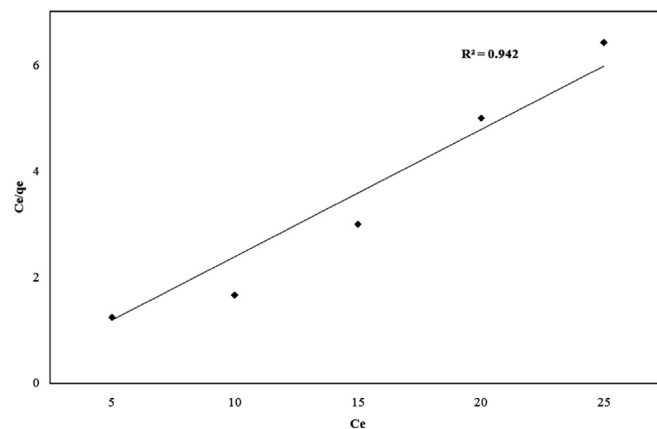


Fig. 6. The linear Langmuir Adsorption Isotherm for phenol with sawdust.

$$\frac{C_e}{q_e} = \frac{1}{Q_0 b} + \frac{C_e}{Q_0} \quad (6)$$

where C_e (mg/L) is the equilibrium concentration of the solution, q_e (mg/g) is the amount of phenol sorbed at equilibrium, Q_0 is the adsorption capacity and represents a practical limiting adsorption capacity when the adsorbent surface is fully covered with monolayer adsorbent molecule and b is Langmuir constant. The Q_0 and b values are calculated from the slopes ($1/Q_0$) and intercepts ($1/Q_0 b$) of the following linear plot of C_e/q_e versus C_e . The straight line indicates that the adsorption complies with the Langmuir model as shown in Fig. 6.

3.1.3. Characterization of adsorbent

Sawdust showed better performance in for phenol adsorption (78.3%). The functional groups responsible for phenol biosorption onto sawdust were studied by FTIR spectra. The FTIR spectroscopy is a significant systematic technique, which identifies the vibration features of functional groups that are available on sorbent surfaces. The result presented in Fig. 7(a) and (b). Peak around the section 2384.12 cm^{-1} and 3214.35 cm^{-1} indicates $-\text{CH}$ and $-\text{OH}$ functional group. A peak observed around 3785.48 cm^{-1} indicates vibration of O-H group (free non-hydrogen bonded). The absorption peaks around 1302.45 cm^{-1} established the occurrence of carboxyl groups in the $\text{CH}_2\text{-OH}$ polysaccharide structure [39]. Peaks at 1257.22 cm^{-1} were the stretching of O-H functional groups. The strong band within $1125\text{--}700 \text{ cm}^{-1}$ is owing to $\text{CH}_2\text{-OH}$ group, which is the representative peak for polysaccharides. The peak around 1525.65 cm^{-1} relates to owing to the occurrence of carboxyl and carbonate structures, conjugated hydrocarbon groups, carboxylic groups and aromatic hydrocarbons, representing biosorption of phenol. The change was the disappearance of peaks at 3785.35 cm^{-1} , 1611.05 cm^{-1} , 1408.20 cm^{-1} , 1145.65 cm^{-1} and 1135.09 cm^{-1} indicating a decrease of $-\text{OH}$, stretch of COOH , C-OH and $\text{CH}_2\text{-OH}$ group on the surface of biosorbent. It is clear from the FTIR analysis that the possible mechanism of biosorption of phenol on sawdust biomass may be owing to appearance and disappearance of functional groups and chemical reactions with sites of biosorbent surface and also due to physical adsorption.

Analysis of the physicochemical composition of sawdust has been done with EDX, which mention in Table 7 and shown in Fig. 8(a) and (b). The analysis shows the presence of carbon, hydrogen, carbohydrate cellulose, hemicellulose, sulphur, lignin, and ash. The peak 35.98%, 22.05% cellulose, 17.8%, 8.45% hemicellulose was observed before and after application sawdust. Ash contents increase in adsorbent from 4.7% to 8.5% wt. after phenol adsorption. Scanning electron micrograph was used to characterize the surface morphology of the sample as shown in Fig. 9(a) and (b). It can be seen from Fig. 9(a) smooth morphology and large pore is available on the sawdust surface. The well-developed pores resulted in the larger surface area and more porous

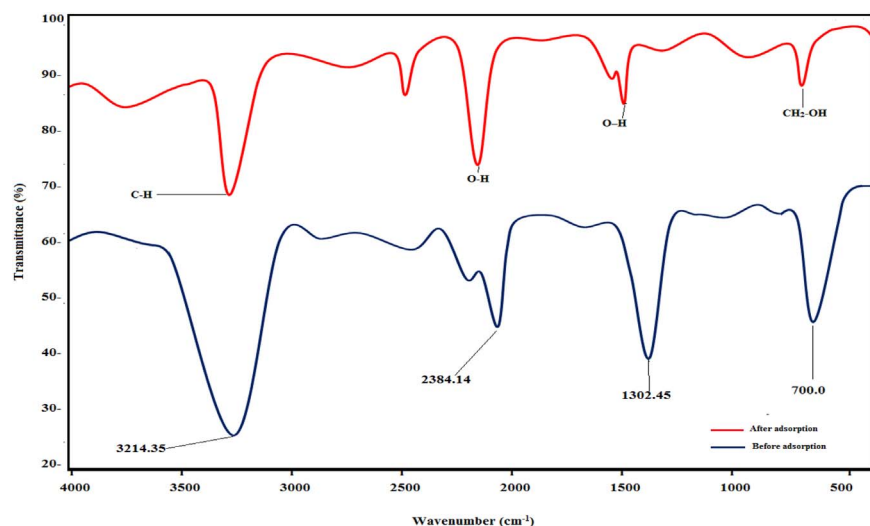


Fig. 7. Fourier transformed infrared study of sawdust (a) before used, (b) after used.

Table 7
Approximate analysis of sawdust.

S.No	Components	Before adsorption (wt %)	After adsorption (wt %)
1	Total volatile matter	85.47	45.34
2	Total carbonate	51.7	30.1
3	Cellulose	35.98	22.05
4	Hemicellulose	17.8	8.45
5	Carbon	45.01	20.65
6	Hydrogen	6.47	2.45
7	Nitrogen	0.29	0.01
8	Sulphur	0.55	0.02
9	lignin	25.4	10.17
10	Ash	4.7	8.5

structure of the SD which would further enhance the adsorption process. Fig. 9(b) shows after adsorption process SD, the porous structure of SD was full of cavities. The surface micrograph appeared like damaged and uneven due to phenol ions adhere on the surface of sawdust. This is assumed to be effective biosorption of phenol onto SD.

3.2. Comparatively, study with others

In literature, a variety of methods has been introduced to handle the phenolic wastewater, such as electrocoagulation [40], advanced oxidation [41], different biological and non-biological methods [42], and biomass waste including with sawdust [43,44]. It was noticed that by electrocoagulation 92% of phenol has been removed at initial concentration 2.5 mg/L, pH 2.0 and treatment time 30 min. Suzuki et al., 2015 reported that 100% decomposition of 50 mg/dm³ phenol was

reached within 120 min using an O₃-UV-TiO₂ process. Another study shows that phenol-degrading bacteria that can utilize 500–600 mg/l phenol completely after 48 h incubation belongs to *Pseudomonas Putida* strains. This technique associated with high-priced treatment, low efficiency, with toxic by-products. Some author has been also reported phenol removal 91.6% at 130 mg/l of initial concentration, 0.82 g of adsorbent dose, natural pH 6.7 and 120 min of contact time [43] and 83% of phenol at initial concentration of 50 mg/L, pH 6, and adsorption 60 min at normal temperature [44]. As compared to all above study present experiment results shows 78.3% adsorption of phenol at the minimum operating condition of initial concentration 10 mg/l, contact time 1.5 h, adsorbent dose 4 g and pH 2. It was found that with a small amount of adsorbent and experimental time, maximum absorptions of phenol have been achieved. Sawdust is easily available nearby local area and cost-effective also. Hence, make use of sawdust as adsorbent will contribute to the sustainability of the surrounding environment.

4. Conclusion

The statistical design of the experiments was applied in optimizing the conditions of maximum adsorption of the phenol onto sawdust. The result data from ANOVA demonstrates that the model was highly significant. For numerical optimization of sawdust, the optimum response result was 78.3%, percentage adsorption at 10 mg/l initial concentration, 1.5 h contact time, 4 g adsorbent dose and pH 2. The quadratic model was found to have maximum Adj R² 0.7223, and Pre R² 0.5739 values. The results of Isotherm data showed that the adsorption of phenol followed Langmuir isotherm. The FTIR spectra give information about the disappearance of functional groups on the surface of the sorbent. Scanning electron micrograph shows the high porous structure

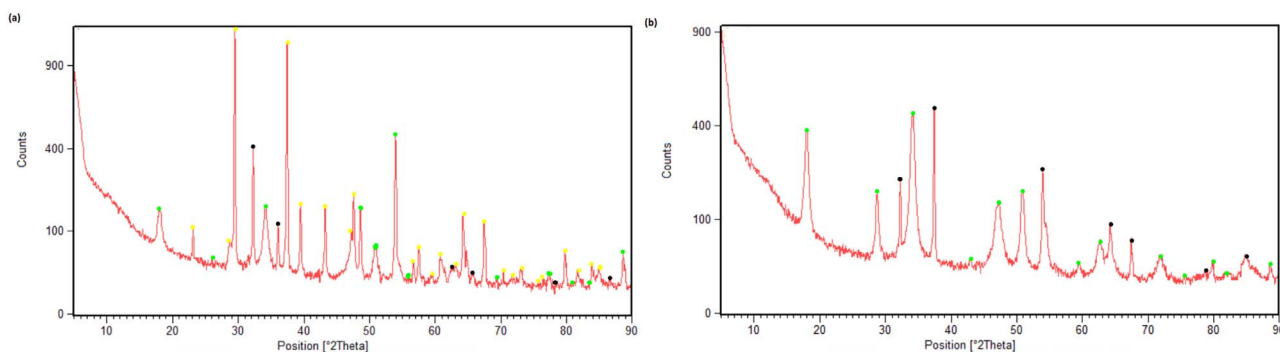


Fig. 8. EDX study of sawdust (a) before used, (b) after used.

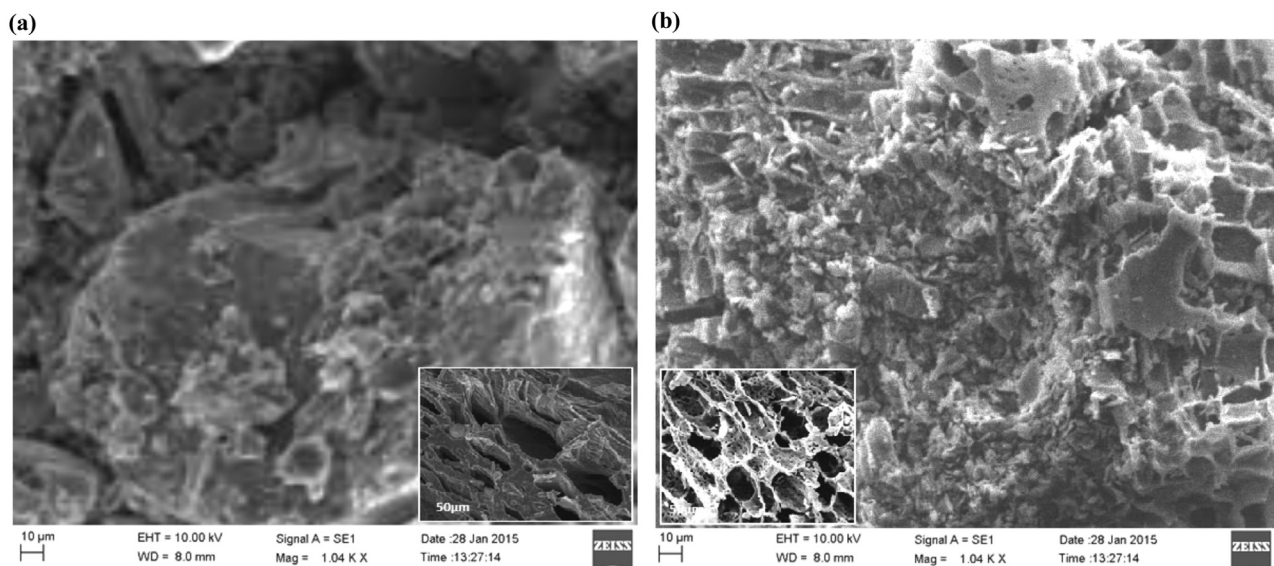


Fig. 9. SEM study of sawdust (a) before used, (b) after used.

of sawdust. After adsorption of phenol, the activated carbon has been washed with warm water (40 °C). The wastewater generated has been used as floor-washing; due to phenol has antimicrobial property (insects and home flies). The activated carbon can be used for cement material or reuse again for adsorption purpose. The outcome of this study proof that biosorbent (activated sawdust) can be used in tertiary treatment for the adsorption of phenol from industrial effluents discharge. The application of response surface methodology gives valuable information on interactions between the factors and also helps to the recognition of possible optimum values of the studied factors.

Appendix A. Transparency document

Transparency document associated with this article can be found in the online version at <http://dx.doi.org/10.1016/j.bbrep.2017.08.007>.

References

- [1] HazDat, HazDat Database: ATSDR'S Hazardous Substance Release and Health Effects Database, Agency for Toxic Substances and Disease Registry, Atlanta, GA, 2006 (www.atsdr.cdc.gov/hazdat.html) (October 14, 2006).
- [2] A.I. Raju, SatyanandamK, Sorption of synthetic bromo phenol blue dye using Gelidium Cartilagineum powder and optimization using central composite design, *Int. J. Emerg. Eng. Res. Technol.* 3 (12) (2015) 109–127.
- [3] M.D. Víctor-Ortega, J.M. Ochando-Pulido, A. Martínez-Ferez Phenols removal from industrial effluents through novel polymeric resins: kinetics and equilibrium studies. <http://dx.doi.org/10.1016/j.seppur.2016.01.023>.
- [4] C. Brage, Q. Yu, G. Chen, K. Sjöström, Tar evolution profiles obtained from gasification of biomass and coal, *Biomass Bioenergy* 18 (1) (2000) 87–91.
- [5] S. Rengaraj, S.H. Moon, R. Sivabalan, B. Arabindoo, V. Murugesan, Removal of phenol from aqueous solution and resin manufacturing industry wastewater using an agricultural waste: rubber seed coat, *J. Hazard. Mater.* 89 (2) (2002) 185–196.
- [6] H.P. Gilfrich, S. Rösinger, H. Wilski, The radiation resistance of thermoset plastics—I. phenolic plastics with inorganic fillers, *Int. J. Radiat. Appl. Instrum. Part C. Radiat. Phys. Chem.* 38 (5) (1991) 431–443.
- [7] J.D. Megiatto, E.C. Ramires, E. Frollini, Phenolic matrices and sisal fibers modified with hydroxy terminated polybutadiene rubber: impact strength, water absorption, and morphological aspects of thermosets and composites, *Ind. Crops Prod.* 31 (1) (2010) 178–184.
- [8] A. Effendi, H. Gerhauser, A.V. Bridgwater, Production of renewable phenolic resins by thermochemical conversion of biomass: a review, *Renew. Sustain. Energy Rev.* 12 (8) (2008) 2092–2116.
- [9] Z. Wen, F. Meng, M. Chen, Estimates of the potential for energy conservation and CO₂ emissions mitigation based on Asian-Pacific Integrated Model (AIM): the case of the iron and steel industry in China, *J. Clean. Prod.* 65 (2014) 120–130.
- [10] O. Yilmaz, I.C. Kantarli, M. Yuksel, M. Saglam, J. Yanik, Conversion of leather wastes to useful products, *Resour., Conserv. Recycl.* 49 (4) (2007) 436–448.
- [11] M. Ugurlu, A. Gürses, C. Dogar, M. Yalçın, The removal of lignin and phenol from paper mill effluents by electrocoagulation, *J. Environ. Manag.* 87 (3) (2008) 420–428.
- [12] M.N.M. Ibrahim, N. Zakaria, C.S. Sipaut, O. Sulaiman, R. Hashim, Chemical and thermal properties of lignins from oil palm biomass as a substitute for phenol in a phenol formaldehyde resin production, *Carbohydr. Polym.* 86 (1) (2011) 112–119.
- [13] W.W. Anku, M.A. Mamo, P.P. Govender, Phenolic Compounds in Water: Sources, Reactivity, Toxicity and Treatment Methods. In *Phenolic Compounds-Natural Sources, Importance and Applications*, InTech, 2017.
- [14] N.A.S. Amin, J. Akhtar, H.K. Rai, Screening of combined zeolite-ozone system for phenol and COD removal, *Chem. Eng. J.* 158 (2010) 520–527.
- [15] A. Ginos, T. Manios, D. Mantzavinos, Treatment of olive mill effluents by coagulation–flocculation–hydrogen peroxide oxidation and effect on phytotoxicity, *J. Hazard. Mater.* 133 (1) (2006) 135–142.
- [16] C. Yang, Y. Qian, L. Zhang, J. Feng, Solvent extraction process development and on-site trial-plant for phenol removal from industrial coal-gasification wastewater, *Chem. Eng. J.* 117 (2) (2006) 179–185.
- [17] M.S.A. Palma, J.L. Paiva, M. Zilli, A. Converti, Batch phenol removal from methyl isobutyl ketone by liquid–liquid extraction with chemical reaction, *Chem. Eng. Process.: Process Intensif.* 46 (8) (2007) 764–768.
- [18] A. Bódalo, E. Gómez, A.M. Hidalgo, M. Gómez, M.D. Murcia, I. López, Nanofiltration membranes to reduce phenol concentration in wastewater, *Desalination* 245 (1) (2009) 680–686.
- [19] M. Caetano, C. Valderrama, A. Farran, J.L. Cortina, Phenol removal from aqueous solution by adsorption and ion exchange mechanisms onto polymeric resins, *J. Colloid Interface Sci.* 338 (2) (2009) 402–409.
- [20] S. Larous, A.-H. Meniai, The use of sawdust as by product adsorbent of organic pollutant from wastewater: adsorption of phenol, *Energy Procedia* 18 (2012) 905–914.
- [21] B. Abussaud, H.A. Asmaly, T.A. Saleh, V.K. Gupta, M.A. Atieh, Sorption of phenol from waters on activated carbon impregnated with iron oxide, aluminum oxide and titanium oxide, *J. Mol. Liq.* 213 (2016) 351–359.
- [22] S. Hokkanen, A. Bhatnagar, M. Sillanpaa, A review on modification methods to cellulose-based adsorbents to improve adsorption capacity, *Water Res.* 91 (2016) 156–173.
- [23] M.A. Atieh, Removal of phenol from water different types of carbon – a comparative analysis, *APCBEE Procedia* 10 (2014) 136–141.
- [24] H.D.S.S. Karunarathne, B.M.W.P.K. Amarasinghe, Fixed bed adsorption column studies for the removal of aqueous phenol from activated carbon prepared from sugarcane bagasse, *Energy Procedia* 34 (2013) 83–90.
- [25] M. Gebresemati, O. Sahu, Sorption of DDT from synthetic aqueous solution by eucalyptus bark using response surface methodology, *Surf. Interfaces* 1 (2016) 35–43.
- [26] N. Dwivedi, C. Balomajumder, P. Mondal, Comparative investigation on the removal of cyanide from aqueous solution using two different bioadsorbents, *Water Resour. Ind.* 15 (2016) 28–40.
- [27] Y. Niu, D. Ying, K. Li, Y. Wang, J. Jia, Fast removal of copper ions from aqueous solution using an eco-friendly fibrous adsorbent, *Chemosphere* 161 (2016) 501–509.
- [28] F. Kazemi, H. Younesi, A.A. Ghoreyshi, N. Bahramifar, A. Heidari, Thiol-incorporated activated carbon derived from fir wood sawdust as an efficient adsorbent for the removal of mercury ion: batch and fixed-bed column studies, *Process Saf. Environ. Prot.* 100 (2016) 22–35.
- [29] B.H. Chai, H.C. Meng, Z.G. Zhao, Q. Huang, X. Fu, Removal of color compounds from sugarcane juice by modified sugarcane bagasse: equilibrium and kinetic study, *Sugar Tech.* 18 (3) (2016) 317–324.
- [30] D.C. Montgomery, *Design and Analysis of Experiments*, 5th ed., John Wiley and Sons, New York, USA, 2001.
- [31] T.Z. Keith, *Multiple Regression and Beyond: An Introduction to Multiple Regression*

- and Structural Equation Modeling, Routledge, 2014.
- [32] F. Ren, R. Zhang, W. Lu, T. Zhou, R. Han, S. Zhang, Adsorption potential of 2, 4-dichlorophenol onto cationic surfactant-modified phoenix tree leaf in batch mode, *Desalin. Water Treat.* 57 (14) (2016) 6333–6346.
- [33] R. Singh, R. Kaur, K. Lal, K.G. Rosin, M. Srivastava, A. Shukla, Optimization of chromium (VI) and copper (II) adsorption on chemically treated sawdust using response surface methodology, *Asian J. Chem.* 29 (4) (2017) 728.
- [34] A. Mahavi, A. Maleki, A. Eslami, Potential of rice husk and rice husk ash for phenol removal in aqueous systems, *Am. J. Appl. Sci.* 14 (2004) 321–326.
- [35] Q. Miao, Y. Tang, J. Xu, X. Liu, L. Xiao, Q. Chen, Activated carbon prepared from soybean straw for phenol adsorption, *J. Taiwan Inst. Chem. Eng.* 44 (3) (2013) 458–465.
- [36] O.A. Ekpote, M. Horsfall, T. Tarawou, Potential of fluid and commercial activated carbons for phenol removal in aqueous systems, *ARPN J. Eng. Appl. Sci.* 5 (9) (2010) 39–47.
- [37] N. Singh, B. Agarwal, C. Balomajumder, Simultaneous treatment of phenol and cyanide containing aqueous solution by adsorption, biotreatment and simultaneous adsorption and biotreatment (SAB) process, *J. Environ. Chem. Eng.* 4 (2016) 564–575.
- [38] I. Langmuir, The Adsorption of Gases on Plane Surfaces of Glass, Mica and Platinum, *J. Am. Chem. Soc.* 40 (9) (1918) 1361–1403, <http://dx.doi.org/10.1021/ja02242a004>.
- [39] C. Gok, D.A. Turkozu, S. Aytas, Removal of Th(IV) ions from aqueous solution using bi-functionalized algae-yeast biosorbent, *J. Radioanal. Nucl. Chem.* 287 (2011) 533–541.
- [40] S. Vasudevan, An efficient removal of phenol from water by peroxi-electro-coagulation processes, *J. Water Process Eng.* 2 (2014) 53–57.
- [41] H. Suzuki, S. Araki, H. Yamamoto, Evaluation of advanced oxidation processes (AOP) using O₃, UV, and TiO₂ for the degradation of phenol in water, *J. Water Process Eng.* 7 (2015) 54–60.
- [42] S. Kumari, D. Chetty, N. Ramdhani, F. Bux, Phenol degrading ability of *Rhodococcus pyridinivorans* and *Pseudomonas aeruginosa* isolated from activated sludge plants in South Africa, *J. Environ. Sci. Health, Part A* 48 (8) (2013) 947–953.
- [43] I.H. Dakhil, Removal of phenol from industrial wastewater using sawdust, *Int. J. Eng. Sci.* 3 (1) (2013) 25–31.
- [44] R.S. Ingole, D.H. Lataye, Adsorptive removal of phenol from aqueous solution using activated carbon prepared from babul sawdust, *J. Hazard. Toxic. Radioact. Waste* 19 (4) (2015) 04015002.